NANO LETTERS

Letter

pubs.acs.org/NanoLett

Structural Transition in Layered $As_{1-x}P_x$ Compounds: A Computational Study

Zhen Zhu, Jie Guan, and David Tománek*

Physics and Astronomy Department, Michigan State University, East Lansing, Michigan 48824, United States

Supporting Information

ABSTRACT: As a way to further improve the electronic properties of group V layered semiconductors, we propose to form in-layer 2D heterostructures of black phosphorus and gray arsenic. We use ab initio density functional theory to optimize the geometry, determine the electronic structure, and identify the most stable allotropes as a function of composition. Because pure black phosphorus and pure gray arsenic monolayers differ in their equilibrium structure, we predict a structural transition and a change in frontier states, including a change from a direct-gap to an indirect-gap semiconductor, with changing composition.

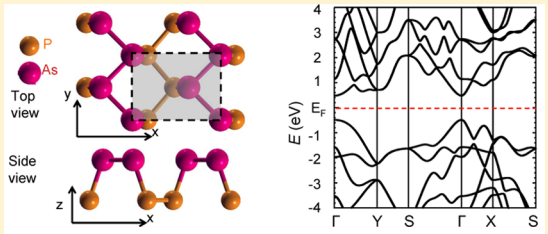

Equilibrium geometry and electronic band structure in an α-$P_{0.5}As_{0.5}$ monolayer

KEYWORDS: *phosphorene, arsenene, compound, ab initio, electronic band structure, structural phase transition*

Few-layer structures of group V elements, including phosphorene and arsenene, are emerging as promising candidates for two-dimensional (2D) electronic materials application.[1−5] Different from semimetallic graphene,[6,7] these systems display a nonzero band gap while still maintaining a relatively high carrier mobility.[3,8−11] Even though phosphorus and arsenic are both group V elements, they crystallize in different structures. Most stable and, thus, more abundant are the layered allotropes such as black phosphorus,[12] with the designation *A*17 or α-P, and gray arsenic,[4] with the designation *A*7 or β-As.[13] Because a conversion of the α (or *A*17) to the β (or *A*7) phase is possible,[14,15] combining both elements in the same layer and changing the composition is bound to cause a structural transition.[16,17] Because both structures are almost equally stable, we may expect phase coexistence that should bring an unexpected richness in both structural and electronic properties.[5,16,18,19] This way of isoelectronic doping could turn into an effective way to fine-tune the electronic properties, increase the carrier mobility,[5] and reduce the chemical reactivity of the compound from those of pristine of phosphorene and arsenene.[20]

In this study, we report ab initio density functional theory (DFT) calculations of $As_{1-x}P_x$ monolayers. We determine the optimum geometry, the electronic structure, and identify the most stable allotropes as a function of composition. We predict a structural transition from the α to the β phase to occur near x = 0.93. This structural transition is accompanied by a change in frontier states from lone pair electron states in α-P to σ-bond states in β-As and from a direct to an indirect fundamental gap.

Results and Discussion. We present in the following computational results for the equilibrium geometry and electronic structure of $As_{1-x}P_x$ compounds as a function of composition. The monolayer structures have been optimized using DFT with the Perdew−Burke−Ernzerhof (PBE)[21] exchange-correlation functional, as discussed in the Methods Section. This approach correctly reproduces the cohesive energy of pristine black phosphorus and gray arsenic.[4,22] Because group V elements phosphorus and arsenic are both 3-fold coordinated and display a tetrahedral bonding character, they possess the freedom to arrange atoms in a layered structure that is not flat, which leads to various buckled allotropes that are topologically related to a honeycomb lattice.[23] Among these, the α and β phases are most stable.[14] Under ambient pressure, phosphorus favors the α and arsenic the β structure, but an $\alpha \rightarrow \beta$ transition has been reported under high pressure.[15,24] As seen in Figure 1a, a monolayer of α-P (black phosphorus) can be viewed as a distorted honeycomb lattice with a rectangular primitive unit cell. The structure of a β-As (gray arsenic) monolayer, presented in Figure 1b, resembles more closely the honeycomb lattice of graphene with a hexagonal unit cell.

We explored the atomic structure of $As_{1-x}P_x$ monolayers in the composition range $0 < x < 1$. In particular, we considered different arrangements of As and P atoms in systems with x = 0.25, 0.5, and 0.75 in the α and β phase. In addition, we also studied compound structures with x = 1/3 and x = 2/3 in the α-phase only. We optimized the lattice structure for each system and found that the lattice constants depend primarily on x and increase with increasing As concentration due to the larger atomic radius of arsenic in comparison to phosphorus. In the strongly anisotropic α phase, we found an increase of 4% along the softer a_1 direction and a 10% increase along the harder a_2 direction when moving from pristine phosphorus to arsenic. The corresponding change in both a_1 and a_2 was an increase by 9% in the isotropic β phase. The data for the

Received: June 5, 2015
Revised: August 20, 2015
Published: August 21, 2015

ACS Publications © 2015 American Chemical Society

DOI: 10.1021/acs.nanolett.5b02227
Nano Lett. 2015, 15, 6042−6046

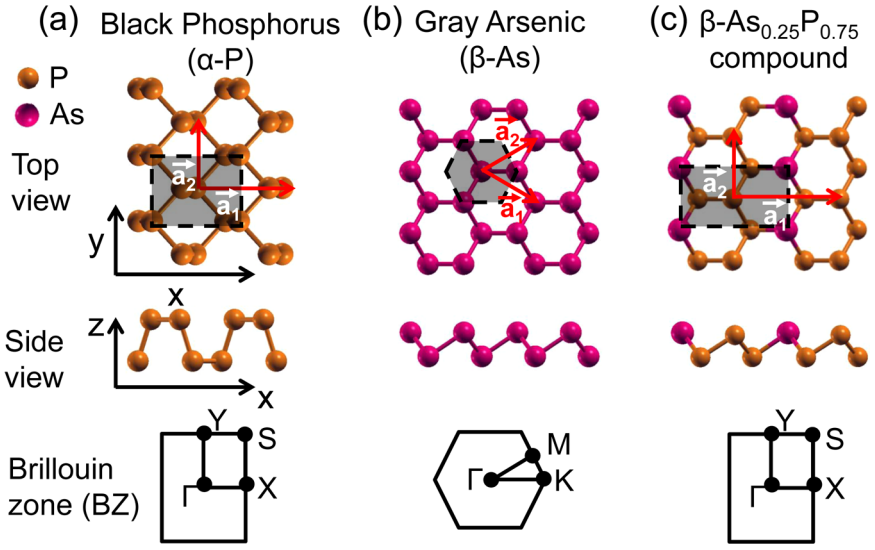

Figure 1. (Color online) Equilibrium structure of a monolayer of (a) black phosphorus (α-P), (b) gray arsenic (β-As), and (c) the β allotrope of the $As_{0.25}P_{0.75}$ compound. Ball-and-stick models in top and side view, with the primitive unit cell highlighted by shading, are shown in the upper panels and the Brillouin zones in the lower panels.

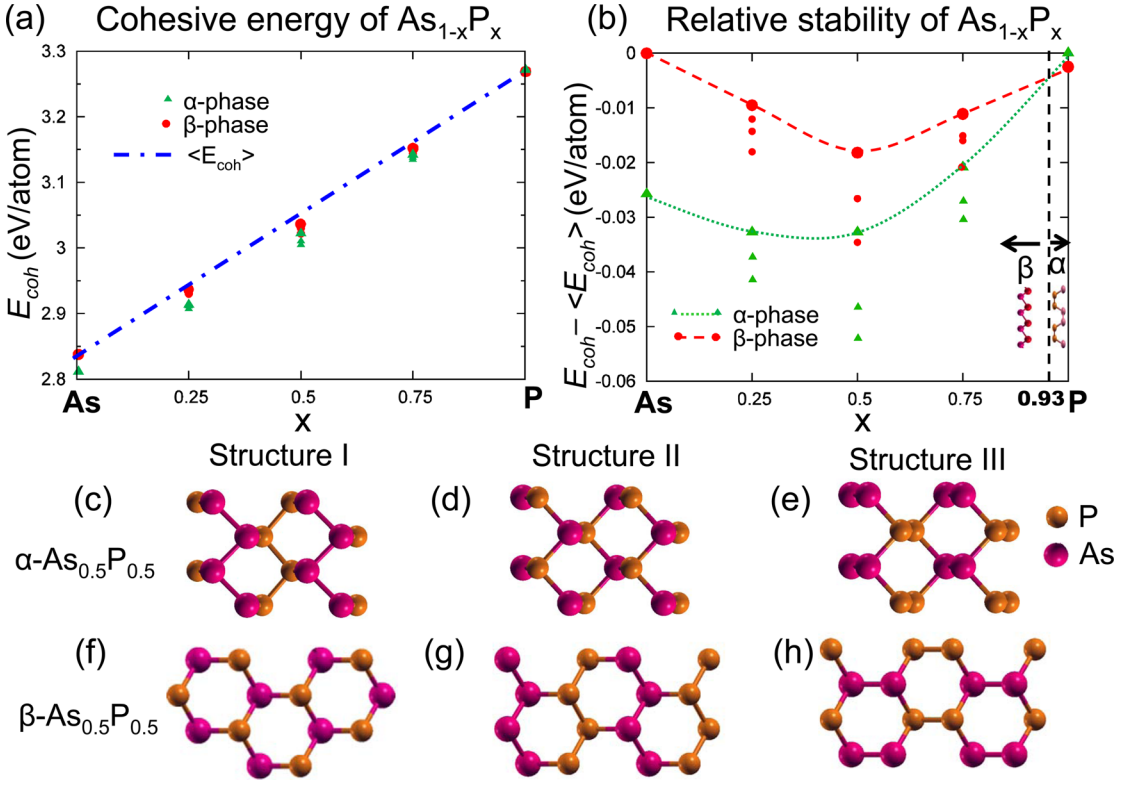

Figure 2. (Color online) (a) Cohesive energy E_{coh} of an $As_{1-x}P_x$ monolayer as a function of the phosphorus concentration x. The most stable allotropes are shown by larger symbols. $\langle E_{coh}\rangle$, shown by the dash-dotted line, is a linear interpolation between the most stable allotropes of As and P. (b) Relative stability $E_{coh}-\langle E_{coh}\rangle$ of $As_{1-x}P_x$ as a function of x. The vertical dashed line indicates the expected composition for an $\alpha \rightarrow \beta$ structural transition. Ball-and-stick models of selected stable structures of $As_{0.5}P_{0.5}$ in the [(c)−(e)] α phase and [(f)−(h)] β phase. For each phase, the structural indices I, II, and III are arranged in the order of increasing stability.

dependence of the lattice parameters on composition are presented in the Supporting Information.

Because the cohesive energy of phosphorus is larger than that of arsenic, we expect a larger cohesive energy in phosphorus-rich structures. In the first approximation, if we were to ignore structural and short-range order differences, we would expect the cohesive energy of the $As_{1-x}P_x$ compound to be a linear combination of the cohesive energies of the pristine components in their respective structures, $\langle E_{coh}\rangle = (1 - x)E_{coh}(\text{As}) + xE_{coh}(\text{P})$. In a compound with a particular structure, we define the cohesive energy per "average atom" by $E_{coh}(As_{1-x}P_x) = -E_{tot}(As_{1-x}P_x)/N + (1 - x)E_{tot}(\text{As atom}) + xE_{tot}(\text{P atom})$, where $E_{tot}(As_{1-x}P_x)$ is the total energy of the N-atom unit cell, $E_{tot}(\text{As atom})$ is the total energy of an isolated

DOI: 10.1021/acs.nanolett.5b02227
Nano Lett. 2015, 15, 6042−6046

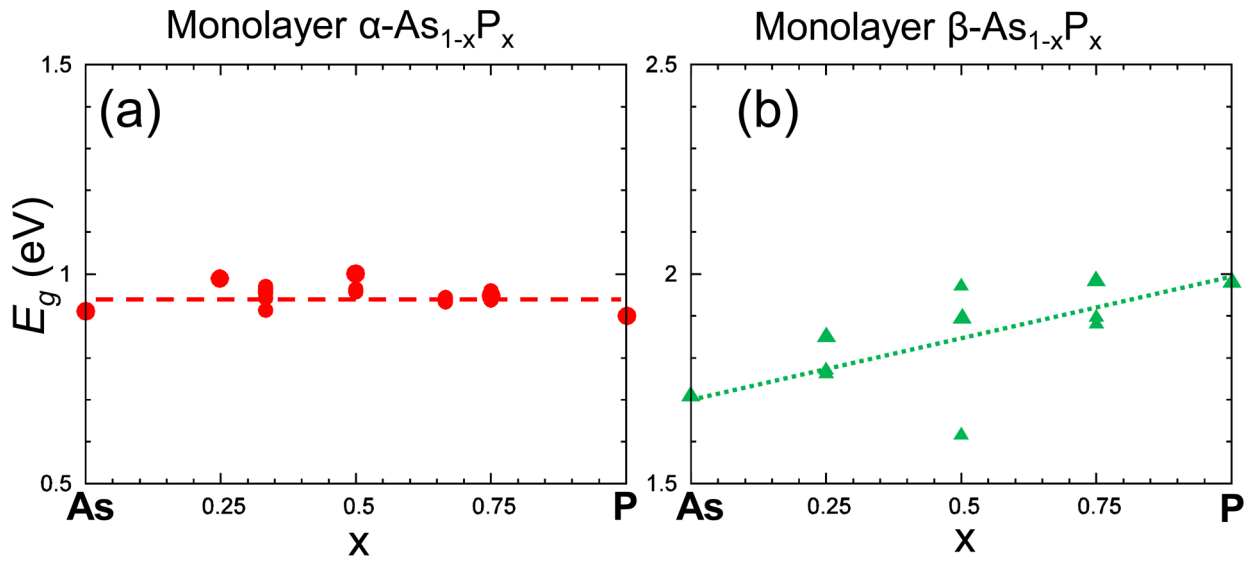

Figure 3. (Color online) Fundamental electronic band gap E_g in $As_{1-x}P_x$ monolayers. DFT-PBE values of E_g are presented as a function of composition for compounds in the (a) α and (b) β phases. The dashed lines are guides to the eye.

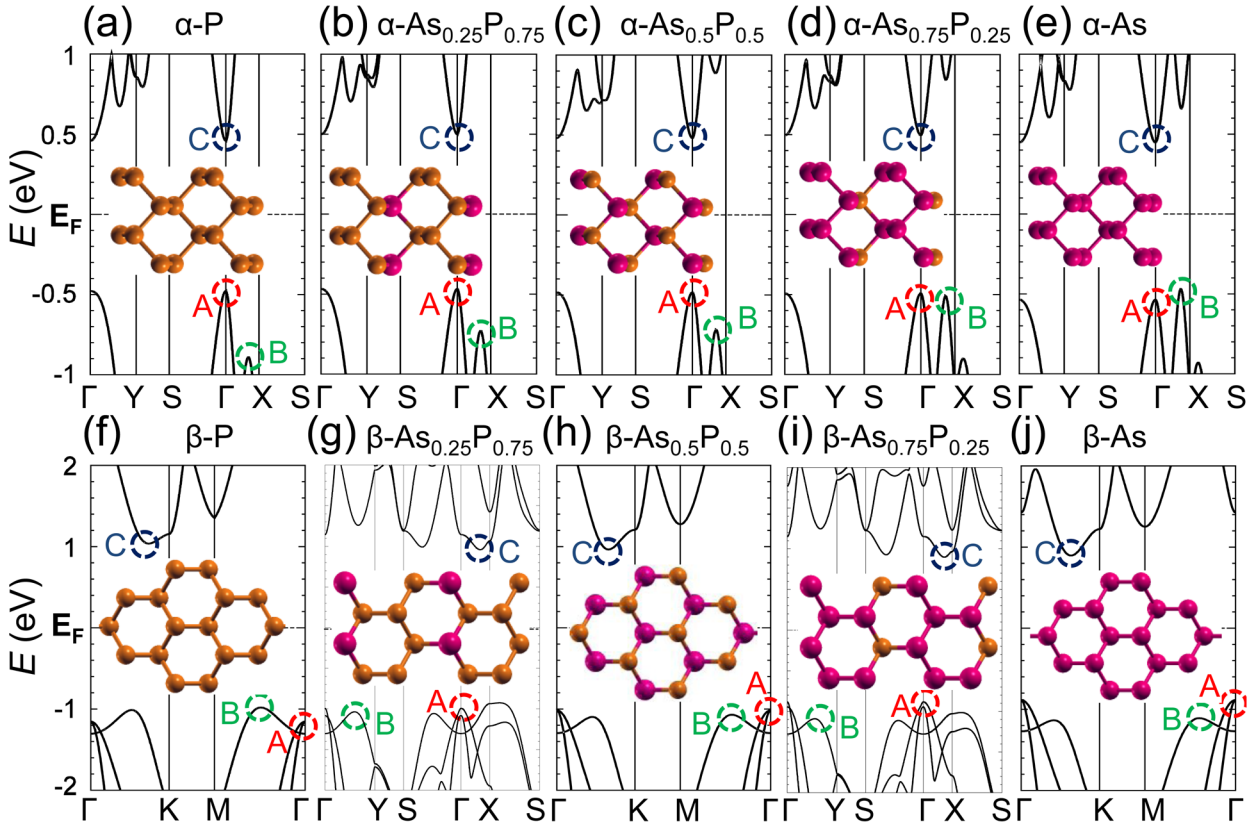

Figure 4. (Color online) Electronic band structure of $As_{1-x}P_x$ monolayers in the α-phase [(a)−(e)] and the β-phase [(f)−(j)]. The structural arrangements for each composition are shown in the insets. The changing role of the valence band maxima, shown by the dashed circles labeled "A" at Γ and "B" off-Γ, is discussed in the text. The position of the conduction band minima is indicated by the dashed circles labeled "C".

As atom and E_{tot}(P atom) the total energy of a P atom. As seen in Figure 2a, the cohesive energy $E_{coh}(As_{1-x}P_x)$ will generally deviate from the expectation value $\langle E_{coh}\rangle$ for specific geometries and atomic arrangements, but the deviations are rather small.

To better investigate these deviations, we define the relative stability of a given structure by $E_{coh}(As_{1-x}P_x) - \langle E_{coh}\rangle$ and show the results in Figure 2b. In general, we find that combining both elements in the same layer is always associated with an energy penalty with respect to the $\langle E_{coh}\rangle$ value, caused by the size mismatch of As and P atoms. For a given composition, we found cohesive energy differences between particular arrangements of As and P atoms to be as large as 20 meV/atom at $x = 0.5$. Because the cohesive energy ranges of the different atomic arrangements within the phases overlap, we expect a coexistence of the two phases in realistic samples.

DOI: 10.1021/acs.nanolett.5b02227
Nano Lett. 2015, 15, 6042−6046

We found the monolayer of β-As to be more stable by ≈26 meV/atom than that of α-As, whereas the monolayer of α-P is favored by ≈3 meV/atom over β-P. As seen in Figure 2b, the energy penalty in the β phase is smaller than that in the α phase for lower x values. Only in very phosphorus-rich compounds we find the α phase to be more stable. Consequently, we expect a structural transition between the α and the β phase to occur as a function of composition. Our results indicate that this structural transition should occur near $x \approx 0.93$, close to the transition observed in bulk $As_{1-x}P_x$ compounds.[16]

To illustrate how the relative position of arsenic and phosphorus atoms affects the stability of the compounds, we present three different structures of $As_{0.5}P_{0.5}$ in the α phase in Figure 2c−e and in the β phase in Figure 2f−h. As the cohesive energy of phosphorus is larger than that of arsenic, P−P bonds are stronger than As−As bonds. Consequently, the structure with the largest number of P−P bonds should be most stable. On the other hand, maximizing the P−P interaction would imply segregating P from As, which will strain the structure. There is a trade-off between the two trends. For the sake of convenience, we called the least stable structural arrangement "structure I" and the most stable arrangement "structure III" in Figure 2. As seen in Figure 2e and h, the two most stable structures in either phase contain an alternating arrangement of isolated P−P and As−As dimers. In this arrangement, the strain caused by different bond lengths can be minimized, while still keeping at least some P−P bonds. Strain is also low in the α-II and β-I structures, but absence of P−P bonds makes them less stable. The largest number of P−P bonds is realized in the α-I and β-II structures, but the large strain energy caused by the coexistence of phosphorus and arsenic chain arrangements makes these structures energetically unfavorable.

As mentioned above, the relatively small stability difference between the α and β phase of $As_{1-x}P_x$ compounds suggests a likely coexistence of different allotropes. Understanding the electronic properties of such a complex system requires obtaining information about every such structural arrangement. We have performed the corresponding calculations and show the fundamental electronic band gap[25] of $As_{1-x}P_x$ compounds as a function of composition in Figure 3. Even though our DFT-PBE band gaps in the systems of interest are underestimated[25] by ≈1.0 eV in comparison with more proper GW self-energy calculations,[26,27] the trends can usually be trusted.

As indicated in Figure 3a, the electronic band gap value of the α phase does not depend sensitively on the phosphorus concentration x and lies in the range between 0.9−1.0 eV. For the β phase of $As_{1-x}P_x$ compounds, the band gap is much larger and its value increases with increasing phosphorus concentration, as seen in Figure 3b. The band gap values not only display a larger value range from 1.6−2.0 eV, but also depend on the relative arrangement of P and As atoms within the unit cell at a given composition.

More interesting than the absolute value of the band gap are changes in the band structure of $As_{1-x}P_x$ compounds caused by changing composition, which should be correctly captured by DFT-PBE. Especially important appears to be the position of the valence band maximum, because these compounds are expected to behave as p-type semiconductors. The band structure of α-phase compounds is shown in Figure 4a for pristine phosphorus, Figure 4e for pristine arsenic, and in Figures 4b−d for intermediate compositions. Careful comparison of these band structure results indicates a transition from a direct gap in α-P to an indirect gap in α-As. For the sake of discussion, we found it useful to identify the valence band maximum at Γ as point "A", another local valence band maximum along the Γ−X line as point "B", and the conduction band minimum at Γ as point "C". With increasing concentration of As, the valence band maximum switches from "A" to "B", with the transition occurring near $As_{0.75}P_{0.25}$ as seen in Figure 4d. Consequently, the character of the fundamental band gap in $As_{1-x}P_x$ compounds in the α phase is expected to change from direct for $x \gtrsim 0.75$ to indirect for $x \lesssim 0.75$. This behavior is reminiscent of the direct-to-indirect gap transition in a pure α-phosphorene monolayer that is induced by tensile in-layer strain and may be rationalized by the fact that the larger atomic radius of As atoms causes such strain. In reality, we find that the relative positions of the "A" and "B" peaks depend not only on the composition, but also the relative arrangement of phosphorus and arsenic atoms. We compare the electronic band structure of different structural arrangements with $x = 0.5$ in the Supporting Information.

The band structure changes in β-$As_{1-x}P_x$ compounds with changing composition are presented in Figure 4f−j. Similar to the α-phase structures discussed above, we label the valence band maximum at Γ as point "A", another local valence band maximum away from Γ as point "B", and the bottom of the conduction band as point "C". Even though—unlike the α-phase compounds—all β-phase structures are indirect-gap semiconductors, the position of the valence band maxima and conduction band minima still changes with composition. There is a change in β-$As_{1-x}P_x$ from the top of the valence band being at "B" in P-rich compounds with $x \gtrsim 0.5$ to "A" at Γ in As-rich compounds with $x \lesssim 0.5$. Similar changes in the valence frontier states have been observed in a pure As monolayer under strain.[4] Also here, we find that point "A" corresponds to in-plane σ-bond states, whereas point "B" corresponds to lone pair electron states,[4] same as in a β-P monolayer. In other words, changing the composition allows to change the character of the frontier states in the valence band region and thus to effectively tune the electronic properties of the system. We wish to point out that changing the character of the frontier states may have a beneficial effect on reducing the chemical reactivity of the system.

In conclusion, we have performed ab initio density functional theory (DFT) calculations of $As_{1-x}P_x$ monolayers in search of ways to further improve the electronic properties of group V layered semiconductors and reduce their chemical reactivity. We have determined the optimum geometry, the electronic structure, and have identified the most stable allotropes as a function of composition. We have found the most stable allotropes to be based on the α (A17) structure of black phosphorus and the β (A7) structure of gray arsenic. Because the stability difference between these two phases is very small, we expect coexistence of α- and β-type structures within a large composition range. On the basis of our results, we expect a structural transition from the α to the β phase to occur near $x = 0.93$. This structural transition should be accompanied by a change in frontier states from lone-pair electron states in α-P to σ-bond states in β-As and from a direct to an indirect fundamental gap.

Methods. Our computational approach to gain insight into the equilibrium structure, stability, and electronic properties of various phosphorene structures is based on ab initio density functional theory as implemented in the SIESTA code.[28] We used periodic boundary conditions throughout the study. We used the Perdew−Burke−Ernzerhof[21] exchange-correlation func-

DOI: 10.1021/acs.nanolett.5b02227
Nano Lett. 2015, 15, 6042−6046

tional, norm-conserving Troullier–Martins pseudopotentials,[29] and a double-ζ basis including polarization orbitals. The reciprocal space was sampled by a fine grid[30] of $8 \times 8 \times 1$ k-points in the Brillouin zone of the primitive unit cell. We used a mesh cutoff energy of 180 Ry to determine the self-consistent charge density, which provided us with a precision in total energy of $\leq$2 meV/atom. All geometries have been optimized by SIESTA using the conjugate gradient method,[31] until none of the residual Hellmann–Feynman forces exceeded 10^{-2} eV/Å.

■ ASSOCIATED CONTENT

Supporting Information

The Supporting Information is available free of charge on the ACS Publications website at DOI: 10.1021/acs.nanolett.5b02227.

Our results for the dependence of the lattice parameters on composition and the dependence of the electronic band structure of $As_{0.5}P_{0.5}$ compounds on the relative arrangement of As and P atoms are presented in the Supporting Information. (PDF)

■ AUTHOR INFORMATION

Corresponding Author

*E-mail: tomanek@pa.msu.edu.

Notes

The authors declare no competing financial interest.

■ ACKNOWLEDGMENTS

We thank Bilu Liu for useful discussions. This study was supported by the National Science Foundation Cooperative Agreement #EEC-0832785, titled "NSEC: Center for High-rate Nanomanufacturing". Computational resources have been provided by the Michigan State University High Performance Computing Center.

■ REFERENCES

(1) Narita, S.; Akahama, Y.; Tsukiyama, Y.; Muro, K.; Mori, S.; Endo, S.; Taniguchi, M.; Seki, M.; Suga, S.; Mikuni, A.; Kanzaki, H. *Physica B +C* **1983**, *117-118*, 422–424.

(2) Maruyama, Y.; Suzuki, S.; Kobayashi, K.; Tanuma, S. *Physica B+C* **1981**, *105*, 99–102.

(3) Liu, H.; Neal, A. T.; Zhu, Z.; Luo, Z.; Xu, X.; Tomanek, D.; Ye, P. D. *ACS Nano* **2014**, *8*, 4033–4041.

(4) Zhu, Z.; Guan, J.; Tománek, D. *Phys. Rev. B: Condens. Matter Mater. Phys.* **2015**, *91*, 161404.

(5) Liu, B.; Köpf, M.; Abbas, A. N.; Wang, X.; Guo, Q.; Jia, Y.; Xia, F.; Weihrich, R.; Bachhuber, F.; Pielnhofer, F.; Wang, H.; Dhall, R.; Cronin, S.; Ge, M.; Fang, X.; Nilges, T.; Zhou, C. *Adv. Mater.* **2015**, *27*, 4423–4429.

(6) Novoselov, K. S.; Geim, A. K.; Morozov, S. V.; Jiang, D.; Zhang, Y.; Dubonos, S. V.; Grigorieva, I. V.; Firsov, A. A. *Science* **2004**, *306*, 666–669.

(7) Zhang, Y.; Tan, Y.-W.; Stormer, H. L.; Kim, P. *Nature* **2005**, *438*, 201–204.

(8) Li, L.; Yu, Y.; Ye, G. J.; Ge, Q.; Ou, X.; Wu, H.; Feng, D.; Chen, X. H.; Zhang, Y. *Nat. Nanotechnol.* **2014**, *9*, 372–377.

(9) Koenig, S. P.; Doganov, R. A.; Schmidt, H.; Castro Neto, A. H.; Özyilmaz, B. *Appl. Phys. Lett.* **2014**, *104*, 103106.

(10) Xia, F.; Wang, H.; Jia, Y. *Nat. Commun.* **2014**, *5*, 4458.

(11) Castellanos-Gomez, A.; Vicarelli, L.; Prada, E.; Island, J. O.; Narasimha-Acharya, K. L.; Blanter, S. I.; Groenendijk, D. J.; Buscema, M.; Steele, G. A.; Alvarez, J. V.; Zandbergen, H. W.; Palacios, J. J.; van der Zant, H. S. J. *2D Mater.* **2014**, *1*, 025001.

(12) Bridgman, P. W. *J. Am. Chem. Soc.* **1914**, *36*, 1344–1363.

(13) The common designation *A*17 for the structure of layered bulk black phosphorus is here substituted by the designation α phase for few-layer systems. Similarly, the common designation *A*7 for the structure of layered gray arsenic is here substituted by the designation β phase for few-layer systems. The alternative nomenclature using Greek characters has been introduced in the literature recently to characterize the many different stable allotropes in few-layer systems.

(14) Zhu, Z.; Tománek, D. *Phys. Rev. Lett.* **2014**, *112*, 176802.

(15) Boulfelfel, S. E.; Seifert, G.; Grin, Y.; Leoni, S. *Phys. Rev. B: Condens. Matter Mater. Phys.* **2012**, *85*, 014110.

(16) Osters, O.; Nilges, T.; Bachhuber, F.; Pielnhofer, F.; Weihrich, R.; Schöneich, M.; Schmidt, P. *Angew. Chem., Int. Ed.* **2012**, *51*, 2994–2997.

(17) Krebs, H.; Holz, W.; Worms, K. H. *Chem. Ber.* **1957**, *90*, 1031–1037.

(18) Kamal, C.; Ezawa, M. *Phys. Rev. B: Condens. Matter Mater. Phys.* **2015**, *91*, 085423.

(19) Zhang, Z.; Xie, J.; Yang, D.; Wang, Y.; Si, M.; Xue, D. *Appl. Phys. Express* **2015**, *8*, 055201.

(20) Burford, N.; Carpenter, Y.-Y.; Conrad, E.; Saunders, C. D. L. *Biological Chemistry of Arsenic, Antimony and Bismuth*; John Wiley & Sons, Ltd: Hoboken, NJ, 2010; pp 1–17.

(21) Perdew, J. P.; Burke, K.; Ernzerhof, M. *Phys. Rev. Lett.* **1996**, *77*, 3865–3868.

(22) Kittel, C. *Introduction to Solid State Physics*, 8th ed.; Wiley: Hoboken, NJ, 2004.

(23) Guan, J.; Zhu, Z.; Tománek, D. *ACS Nano* **2014**, *8*, 12763–12768.

(24) Jamieson, J. C. *Science* **1963**, *139*, 1291–1292.

(25) DFT calculations are designed to determine the charge distribution and total energy, not the electronic band structure. Interpreting Kohn–Sham eigenvalues $E(\mathbf{k})$ as quasiparticle energies leads to significantly underestimated fundamental band gaps. Comparison with more proper quasiparticle calculations, for example, using a computationally more involved the GW formalism, suggests that the main difference between DFT and GW band structures is a rigid band offset, effectuated by a "scissor operator", which increases the band gap energy, but does not modify much the band dispersion within the valence and conduction bands. Thus, the locations of valence band maxima and conduction band minima in the Brillouin zone, obtained by DFT, can be trusted.

(26) Tran, V.; Soklaski, R.; Liang, Y.; Yang, L. *Phys. Rev. B: Condens. Matter Mater. Phys.* **2014**, *89*, 235319.

(27) Wang, X.; Jones, A. M.; Seyler, K. L.; Tran, V.; Jia, Y.; Zhao, H.; Wang, H.; Yang, L.; Xu, X.; Xia, F. *Nat. Nanotechnol.* **2015**, *10*, 517–521.

(28) Artacho, E.; Anglada, E.; Dieguez, O.; Gale, J. D.; Garcia, A.; Junquera, J.; Martin, R. M.; Ordejon, P.; Pruneda, J. M.; Sanchez-Portal, D.; Soler, J. M. *J. Phys.: Condens. Matter* **2008**, *20*, 064208.

(29) Troullier, N.; Martins, J. L. *Phys. Rev. B: Condens. Matter Mater. Phys.* **1991**, *43*, 1993–2006.

(30) Monkhorst, H. J.; Pack, J. D. *Phys. Rev. B: Condens. Matter Mater. Phys.* **1976**, *13*, 5188–5192.

(31) Hestenes, M. R.; Stiefel, E. *J. Res. Natl. Bur. Stand.* **1952**, *49*, 409–436.

DOI: 10.1021/acs.nanolett.5b02227
Nano Lett. 2015, 15, 6042–6046